# Study of the mechanical behavior of heterogeneous granular materials by means of distinct element method

**Bastien CHEVALIER***
**Gaël COMBE**
**Pascal VILLARD**
*Université de Grenoble, Laboratoire sols, solides, structures – risques, France*

Despite the fact that so-called heterogeneous granular materials are frequently employed in civil engineering applications, their mechanical behavior has only been examined in a few comprehensive studies, whether this be experimentally or numerically. This lack of preliminary investigation could prove problematic especially when it comes to structural design. A two-dimensional, discrete element numerical model has been implemented in order to carry out a systematic study of various types of granular assemblies; this set-up will be composed of two particle families, either in variable proportions or with a relatively tighter particle size distribution. The microstructure of granular assemblies submitted to isotropic confinement has been described in terms of porosity and granular arrangement, and the mechanical behavior of such assemblies was obtained by exposure to biaxial loading. The main parameters studied herein are: the Young's modulus and Poisson's ratio for elastic characteristics, macromechanical angles of friction at both the peak state and within the domain of large deformations, as well as dilatancy using volumetric variation curves vs. axial deformation.

## Étude du comportement mécanique de matériaux granulaires hétérogènes par simulations numériques discrètes

RÉSUMÉ

*Bien que les matériaux granulaires, dits hétérogènes, soient fréquemment utilisés en génie civil, leur comportement mécanique n'a fait l'objet que de peu d'études exhaustives, tant sur le plan expérimental que numérique, ce qui peut s'avérer problématique notamment lorsque l'on souhaite dimensionner des ouvrages. Un modèle numérique par éléments discrets en deux dimensions a été mis en œuvre pour permettre une étude systématique de différents types d'assemblages granulaires : assemblages constitués de deux familles de particules, soit en proportions variables, soit à granulométries plus ou moins resserrées. La microstructure des assemblages granulaires sous confinement isotrope a été décrite en termes de porosité et d'arrangement granulaire. Le comportement mécanique de ces assemblages a été obtenu sous sollicitation biaxiale. Les principaux paramètres étudiés sont le module d'Young et le coefficient de Poisson pour les caractéristiques élastiques, les angles de frottement macromécaniques au pic et dans le domaine des grandes déformations ainsi que la dilatance au travers des courbes de variation de volume en fonction de la déformation axiale.*

**CORRESPONDING AUTHOR:**
**Bastien CHEVALIER**
bastien.chevalier@ujf-grenoble.fr

## INTRODUCTION

Heterogeneous granular materials are, for obvious economic reasons, becoming more frequently used in the field of civil engineering (site materials, crushed aggregates or coarse granular soils). The absence of information on the mechanical behavior of these materials is very real, which creates some serious problems in designing structures that utilize such materials.

The lack of knowledge regarding the behavior of heterogeneous granular materials becomes even more acute when, as in the large majority of cases, mechanical tests conducted in the laboratory require segmenting the particle size range, for obvious material concerns. It is thus important to evaluate the consequences of this experimental approach, which prove critical to estimating the properties of these types of soils.

The numerical and experimental studies conducted for the purpose of determining the behavior of granular materials focus primarily on model materials with continuous **[1]**, or even isometric **[2]**, particle size ranges that do not *a priori* allow assessing the behavior of certain materials with more complex size distributions (e.g. flat, discontinuous). "Laboratory" sands, such as Hostun **[1,3]** or Fontainebleau **[4]**, could be cited herein as could glass beads **[5]**.

This exploratory study is intended to examine the influence of the particle size distribution of heterogeneous granular materials on their mechanical behavior; it was carried out using discrete numerical models that enable running a large number of simulations through implementing systematic and controlled procedures. The numerical simulations were performed on a two-dimensional granular model based on the PFC$^{2D}$ code developed by Itasca **[6]**. The numerical characterization of this type of material by means of a discrete method serves to complement the results obtained from experimental studies and in particular the triaxial testing campaign on glass bead assemblies with variable size distributions conducted by Philippe Reiffsteck at the LCPC laboratory **[4]**.

## GENERAL REMARKS ON HETEROGENEOUS GRANULAR MATERIALS

Heterogeneous granular materials are assemblies of particles or grains, with shapes of varying complexity, and composed of particle families distinguished by their size characteristics: average radius, tightly or loosely compacted radius distribution, etc. The combination of several of these families can in turn be described by means of comparing various types of particles within the mix: number of particle families, ratio of average radii, percentage of each family within the mix, magnitude of granulometric discontinuities.

The diversity of heterogeneous granular materials is therefore quite vast, and this article will focus more narrowly on mixes containing just two types of grains (i.e. bimetric materials), composed of cylindrical particles with circular cross-sections (two-dimensional modeling).

The description of these media under isotropic confinement makes it possible to identify the set of physical phenomena of interest regarding the state of porosity, coordination number (average number of contact points per particle), or actual contact orientation.

### ■ Characterization of porosity

Porosity, which serves to define the relative volumetric share occupied by voids within a given material, is expressed as:

$$\eta = \frac{V_v}{V_s + V_v} \qquad (1)$$

where $V_s$ and $V_v$ represent the solid part volume and the void volume respectively within a given sample.

The description and prediction of granular mix porosity of two particle families were developed in depth, on both theoretical and experimental models **[7-10]**. The porosity prediction of granular mixes has been based on a physical modeling of interparticle voids adapted to heterometric materials, which as a result focuses on the ratio of characteristic radii in each family.

## › Physical modeling of interparticle voids

Porosity variations vs. the proportion of each particle category in a binary mix were established on the basis of a highly-idealized description of an assembly **[7]**. The sample is described as a set of triangular cells (hence a two-dimensional description) obtained by connecting the centers of three adjacent particles. The bold hypothesis adopted regarding this medium is its assumed high density. Only those cells where each particle lies in contact with its two neighboring particles has thus been considered in this set-up (these cells are shown in solid lines in **Fig. 1** below). Consequently, all cells formed by three neighboring yet non-connecting particles are ignored (these cells are shown with dashed lines in **Figure 1**).

It then follows from this modeling arrangement that a cell generated from three same-sized particles will be associated, out of purely geometric considerations, with a porosity that remains higher than that associated with a cell stemming from differently-sized particles. An extension to spherical bimetric mixes yields the porosity curves in **Figure 2** for large-to-small particle diameter ratios ranging from 1.4 to 6.

It can be observed from these curves that Dodds' model **[7]** predicts a systematically lower porosity for bimetric assemblies than for monometric ones. The minimum porosity is reached for a small particle volume ratio varying between 50% and 20% with the diameter ratio lying between 1.4 and 6.

Even if these observations provide a satisfactory estimation of porosity variations in such granular assemblies, they cannot closely depict an actual material in which the shapes of interparticle voids are much more complex.

## › Size ratio

As shown on **Figure 2**, the average particle radius ratios for each family exert a considerable influence on porosity variations within this type of assembly. The addition of a few smaller or larger

**figure 1**
*Triangular cells within a two-dimensional granular medium (according to reference* **[7]***)*

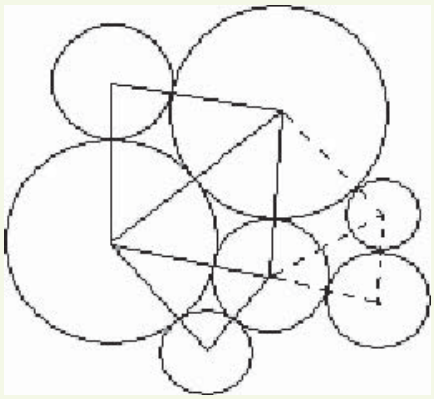

**figure 2**
*Porosity variation vs. bimetric mix proportions for several diameter ratios (3D case) (according to* **[7]***)*

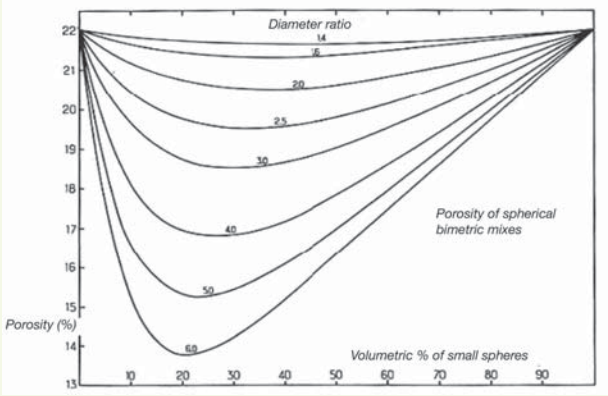

particles in a given assembly of same-sized particles incites modifications to the granular arrangement and, consequently, to the porosity state of the sample.

An insertion mechanism has been demonstrated in the case where a few smaller-sized particles are added to the assembly **[9]**. Depending on the radius ratio between large and small particles, smaller particles may be inserted into the preexisting interparticle void network with or without disturbing the initial granular arrangement. This threshold ratio $\alpha$ equals:

$$\alpha_{2D} = \frac{\sqrt{3}}{2-\sqrt{3}} = 6,46 \quad \textbf{(2)}$$

in the case of (2D) disc assemblies, and equals:

$$\alpha_{3D} \frac{\sqrt{2}}{\sqrt{3}-\sqrt{2}} = 4,45 \quad \textbf{(3)}$$

in the case of (3D) spherical assemblies.

Once this radius ratio drops below the threshold ratio $\alpha$, adding a few smaller particles will disturb the existing particle network **(**see **Fig. 3)** and incite the formation of new triangular cells in the two-dimensional case.

a | b

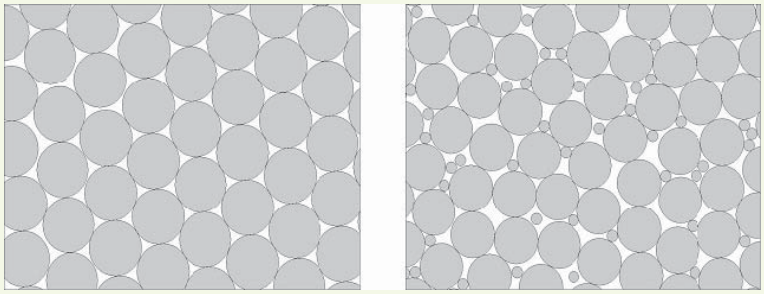

**figure 3**
*Sample of discs submitted to isotropic confinement: (a) case of a homometric mix, and (b) case of a bimetric mix with a 90% large particle volume, for a radius ratio of 4 (i.e. less than $\alpha_{2D}$)*

This particle distribution does not correspond with Dodds' theoretical model (hypothesis of a dense medium) **[7]** and in this specific case, a porosity variation opposite that predicted by the model can actually be anticipated. The additional particles are in effect disturbing the larger particle arrangement and their relative sizes act to prevent the formation of triangular cells whose three particles (in 2D) display two-by-two contact.

Conversely, since the average radius ratio for both families exceeds the threshold ratio $\alpha$, it could be expected that adding a few smaller-sized particles would cause filling of the interparticle void network, which proves to be true as long as the volume of small elements remains less than the volume of voids initially present.

The ancillary mechanism, called the substitution mechanism, is observed upon adding a few particles into an initial assembly of smaller particles. This process entails substituting a single larger element for a given number of smaller elements and their associated voids. The first consequence of this substitution step is to reduce porosity as a result of replacing a number of interparticle voids by a larger particle. The second and opposite effect is to increase porosity due to the interaction between the larger particle and its neighboring smaller ones. Depending on the radius ratio between particles, the combination of these two effects causes either an increase (low radius ratio) or decrease (high radius ratio) in porosity.

Moreover, the effect of substitution on porosity proves more sensitive when the proportion of particles introduced remains limited. In this case, the "inclusions" are embedded into the matrix of smaller particles **(Fig. 4)** and are not in contact with one another.

**figure 4**
*Sample of discs submitted to the isotropic confinement of a bimetric mix with a 10% volume of large particles, for a radius ratio of 4 (less than $\alpha_{2D}$)*

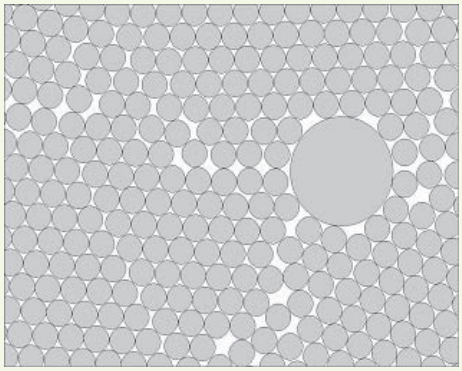

In conclusion, the minimum porosity of a homometric granular material can be reduced by including an additional differently-sized family in an equivalent volume proportion. This porosity will drop even further as the radius ratio characterizing these two families rises.

## Characterization of the granular arrangement

The coordination number *Z* represents the average number of contacts experienced by a single particle within a granular mix. This indicator is useful in providing an accurate description of a sample contact network, which proves to be a basic characteristic of granular materials.

Within a heterometric medium, several types of contacts are found: between two large particles, between two small particles, or between a small and large particle. Besides a global coordination number, four partial coordination numbers are also available: average number of contacts for a small particle in the presence of large particles, for a large particle in the presence of small ones, for large particles among themselves, and for small particles among themselves.

Many studies have been conducted in order to develop coordination number prediction models **[7, 11-13]**. Such models however do not enable accurately and systematically predicting the coordination number distributions. Similarly, the correlation between porosity and coordination number cannot be established. All of these studies taken together reveal that the number of factors involved in the observed variations is substantial. For example, introducing elements into the sample (pluviation, compression, coarsening, lubrication or not, etc.) prohibits any type of comparison, even qualitative. Two major results can nonetheless be mentioned **[13]**. The first is of statistical significance. As the proportion of a given family increases, the number of contacts involving this particular family naturally rises as well. The second is geometric: a larger particle will be associated with a higher average coordination number through being in contact with smaller particles. An increase in the partial coordination number can often be observed however among larger elements as a function of the small element proportion. The geometric effect is more significant for larger particles.

It would thus seem difficult, when using any particular approach for setting elements within a granular assembly, to compare the coordination numbers obtained with those found in the literature. This characteristic specific to granular materials remains fundamental and does influence the mechanical response of these materials.

In order to estimate the influence of microstructure on the behavior of granular materials, experimental compression tests (both biaxial and triaxial) were conducted on steel bead assemblies **[5]**. Even though the tested samples exhibit crystalline arrangements (cubic with centered faces, rhombohedral) that are not representative of granular material arrangements, it was still observed that the material characteristic became more pronounced as the coordination number rose.

## THE STUDIED GRANULAR MODEL

### Discrete numerical modeling methods

The discrete numerical modeling of granular materials has been pursued in a considerable number of studies over the past several decades. The benefit of this type of modeling lies in being able to incorporate a fundamental characteristic of the granular media, i.e. the presence of a set of particles evolving with changes in the level of imposed loadings, featuring both contact losses and contact generation between particles.

Even though interparticle contact laws are difficult to grasp for real materials, discrete numerical simulation serves, in conjunction with the implementation of relatively simplified contact laws, to reproduce the macromechanical behavior of actual granular materials.

The numerical simulations presented below were performed using the PFC$^{2D}$ software **[6]**, which is based on a numerical method classically called "molecular dynamics" **[14]**. This approach makes use of a temporal discretization of the fundamental dynamic relation applied to each particle according to a (conditionally stable) explicit "leapfrog"-patterned diagram **[15]**.

The moving particles interact via two normal and tangential contact laws defined below:

**Normal contact force:** Given two particles numbered *i* and *j* **(Fig. 5)**; the normal contact force $F_N$ is defined by

$$F_N = -k_N h \,,$$

where $k_N$ is the normal contact stiffness and $h$ denotes the interpenetration at contact

$$\text{with} \quad h = \left\| \vec{r}_i - \vec{r}_j \right\| - R_i - R_j \qquad \textbf{(4)}$$

with: $\vec{r}_i$ and $\vec{r}_j$ the center of gravity coordinates of the two particles, and $R_i$ and $R_j$ their respective radii.

**Tangential contact force:** This corresponds to the model proposed by Cundall and Strack **[15]** and correlates the tangential force increment with the relative tangential displacement increment between the two particles in contact via a tangential stiffness $k_T$ over time **(**see **Fig. 5)**. The tangential force is bounded by a Coulomb type friction criterion with coefficient $\mu$. For purposes of our simulations, a zero cohesion has been included in the description of contacts between the modeled particles. If contact between two particles exists at time $t_1$ and persists until time $t_2 = t_1 + \delta t$, then:

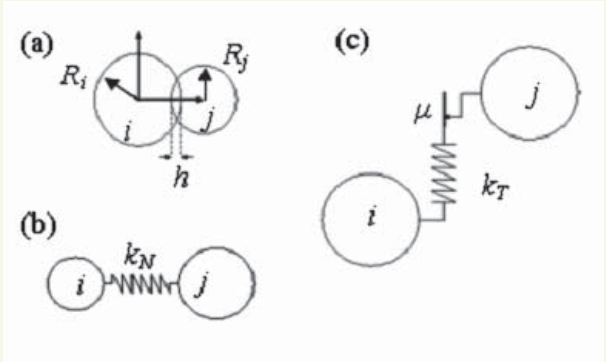


**figure 5**
*Schematic diagram of the normal and tangential interparticle contact laws, along with associated parameters: (a) Contact between particles* i *and* j*, as revealed by their interpenetration* h*; (b) Rheological schematic diagram of the normal contact between* i *and* j*; (c) Rheological schematic diagram of the tangential contact between* i *and* j

$$F_T^{t2} = F_T^{t1} + \delta F_T \quad \text{with} \quad \delta F_T = -k_T.\delta U_T \tag{5}$$

$$\text{and if } \left|F_T^{t2}\right| > \mu F_N^{t2} \quad \text{then:} \quad F_T^{t2} = -\mu F_N^{t2}.\frac{v_T}{|v_T|} \tag{6}$$

where $v_T$ designates the relative tangential velocity of the two particles.

The method employed adopts a local damping introduced into the basic dynamics equations applied to each particle:

$$F_{(i)} + F_{(i)}^d = m_{(i)}A_{(i)} \text{ where } F_{(i)}^d = -\alpha\left|F_{(i)}\right|\text{sign}\left(V_{(i)}\right) \quad \text{with } i = 1\ldots3 \tag{7}$$

$F_{(i)}$, $F_{(i)}^d$, $m_{(i)}$, $A_{(i)}$ and $V_{(i)}$, represent respectively (for $i = 1,2$) the external forces applied to a particle, damping forces, mass, the velocity and acceleration within the two plane directions, and (for $i = 3$) the moment of external forces applied to a particle, damping moment, moment of inertia, the angular velocity and angular acceleration.

The damping coefficient $\alpha$ is equal to 0.7 for the simulations run. This type of local damping does not play a significant role at the level of the mechanical response of the studied assemblies whenever these assemblies are composed of frictional particles and the loading pattern can be considered as quasi-static (which is the present case).

## Micromechanical parameters of the model material

The set of micromechanical parameters used for the numerical simulations are as follows:

$$k_N = 3.10^8\, N.m^{-1}; \quad \frac{k_T}{k_N} = 0,75; \quad \mu = 0,75$$

The apparent level of material stiffness may be evaluated by introducing an adimensional coefficient $\kappa$ **[16-18]** that characterizes a level of interpenetration between particles:

$$\kappa = \left(\frac{h}{2\langle R\rangle}\right)^{-1} \tag{8}$$

where $h$ represents interpenetration at the contact defined in (4) and $\langle R\rangle$ the average radius of a particle. In two dimensions, this adimensional coefficient is replaced by:

$$\kappa = \frac{k_N}{P} \tag{9}$$

where:

$k_N$ is the normal stiffness of the contact law being considered,

$P$ is the 2D confinement pressure (force divided by a length) applied to the samples (100 kPa in the case of the simulations performed herein, given the convention adopted of proceeding by linear meter in the direction perpendicular to the discs).

The simulated granular material displays a stiffness level of $\kappa = 3{,}000$. A number of $\kappa$ values used by various authors have been catalogued **[16,17]**. A coefficient $\kappa = 500$ may be associated with the packing of (2D) wooden cylinders 6 cm long exposed to a confinement of 50 kPa **[19]**; moreover, a (3D) assembly of glass spheres confined under 100 kPa of pressure can be associated with a coefficient $\kappa = 6{,}000$ **[20]**.

A high intergranular friction coefficient ($\mu = 0.75$) was initially adopted to enable a quantitative comparison of numerical results with results obtained experimentally on glass beads **[4]**.

## Methodology

One of the factors influencing the granular packing configuration, as well as the corresponding mechanical responses, is the mode of particle placement. It should be noted that the current array of particle placement techniques practiced is quite broad, in both laboratory experiments and numerical simulation exercises (pluviation, vibration, etc.). To model biaxial tests on dense granular materials, it was preferred to place particles by means of coarsening without friction. Such a procedure allows obtaining assemblies whose porosity is minimized, hence of the same relative density $D_R$ = 1, to be denoted in the following discussion as samples with a "fixed $D_R$ value":

$$D_R = \frac{e - e_{\max}}{e_{\min} - e_{\max}} = \frac{(\eta - \eta_{\max})(1 - \eta_{\min})}{(\eta_{\min} - \eta_{\max})(1 - \eta)} \quad \textbf{(10)}$$

with: $e$ the void index, $e_{max}$ maximum void index, and $e_{min}$ minimum void index,

$\eta$ the porosity, $\eta_{min}$ minimum porosity, and $\eta_{max}$ maximum porosity.

In order to evaluate the density index of samples, a determination was made, in addition to the minimum porosities, of the maximum porosities $\eta_{max}$ of each sample by assuming that these maximum values are found at the critical state (i.e. threshold of the volumetric deformation vs. axial deformation curve) at the time of the biaxial test. This porosity depends on the sample's level of confinement during biaxial crushing and is thus not an intrinsic characteristic of the granular assembly; nonetheless, all simulations discussed herein were run at a constant confinement level ($\sigma_3 = 100\ kPa$).

To generate a set of new samples displaying, from one sample to the next, identical porosity values (denoted samples with a "fixed η value"), it was preferred to proceed with particle placement by means of coarsening with friction. The samples have in fact been derived by considering an initial nonzero coefficient of friction that gets reduced during coarsening until obtaining the desired porosity level.

The samples separated by four partitions have a slenderness ratio of 1 and a constant number of particles. Each sample contains approximately 13,000 particles with variations of between +/-0.2% and +/-3.5%, depending on the specific sample series.

The normal stiffness $k_N$ of contacts between discs and partitions is identical to that considered between two discs. The partition/disc contacts are non-frictional ($\mu = 0$).

Following an isotropic confinement ($\sigma_3 = 100\ kPa$), the samples were subjected to biaxial crushing at a constant deformation speed **(Fig. 6)**.

**figure 6**
*Schematic diagram of the biaxial test - Direction 1 shows the sample crushing direction*

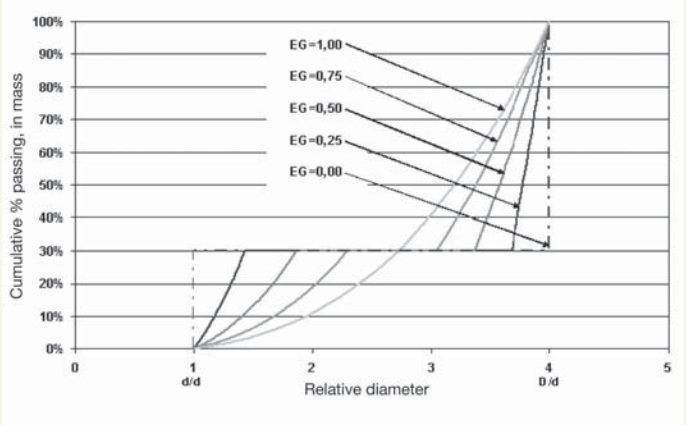

## Particle size distribution parameters

The assemblies under study are bimetric mixes composed of two particle families denoted "fine particles" for discs of small diameter ($d$) and "coarse particles" for large-diameter ($D$) discs. The micromechanical characteristics of these two particle families remain identical. The ratio between the largest and smallest diameters is set at 4 for all samples. An initial series of samples stems from the mix using variable proportions of two perfectly-homometric materials, i.e. all particles of a given type have an identical diameter. Only the mass proportion of each particle family varies. In the following discussion, the mass proportion of coarse particles in the mix will be called $p$. The second series of samples is also constituted of mixes from two particle types. The mass proportion of each type within the sample remains constant ($p = 70\%$). The variable parameter in these samples is the particle distribution spread for each of the two families composing the bimetric granular mix. Each particle family is defined by a uniform granulometric distribution in terms of number of radii over the interval $[d;d']$ for the first and $[D';D]$ for the second. The granular spread (denoted $EG$) can thus be defined as:

$$EG = \frac{(D - D') + (d' - d)}{D - d} \qquad (11)$$

An assembly featuring a uniform particle size distribution between $d$ and $D$ would possess a granular spread of 1, whereas a bimetric assembly in which each component family contains same-sized particles has a granular spread equal to 0.

The size distribution curves for these samples are shown in **figure 7**.

**Table 1** below will summarize the geometric parameters associated with the set of numerical simulations performed.

**figure 7**
*Particle size distribution curves of numerical samples with a variable granular spread*

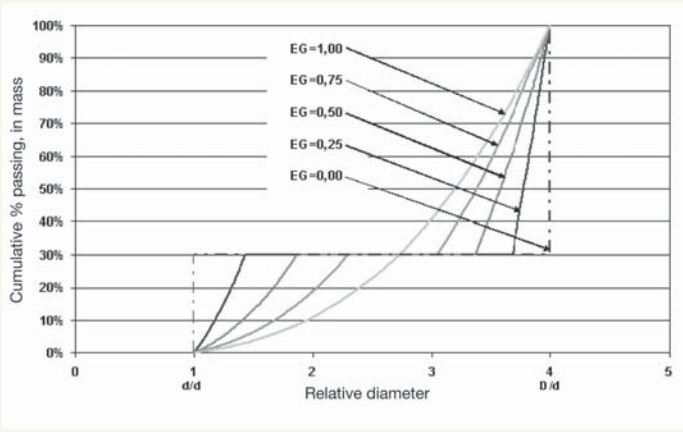


## INFLUENCE OF *P* PROPORTIONS WITHIN THE BIMETRIC MIXES

The initial state (isotropic confinement) of a granular assembly before loading is key and cannot be dissociated from the observed mechanical response within the sample. For this reason, the impetus at first is to describe the initial state of the studied bimetric granular assemblies (i.e. $EG = 0$) prior to focusing on their mechanical response during the biaxial test.

## Characterization of the initial state (isotropic confinement)

### 4.1.1 Study of porosity $\eta$

The variation in porosity, as obtained by isotropic confinement without friction (minimum porosity $\eta_{min}$), vs. the proportion $p$ of coarse particles in the mixes has been depicted in **Figure 8** below.

**tableau 1**
*Summary of the parameters associated with the numerical simulations run*

| Sample designation | $R_{max}/R_{min}$ | Mass percentage of coarse elements *p* | Granular spread *EG* | Total number of particles | Number of samples with a fixed $D_R$ | Number of samples with a fixed $\eta$ |
|---|---|---|---|---|---|---|
| P000EG000 | 4 | 0 | 0.00 | 12.551 | 1 | |
| P010EG000 | 4 | 10 | 0.00 | 12.550 | 1 | |
| P020EG000 | 4 | 20 | 0.00 | 12.999 | 1 | |
| P030EG000 | 4 | 30 | 0.00 | 12.999 | 3 | 1 |
| P040EG000 | 4 | 40 | 0.00 | 12.997 | 3 | 1 |
| P050EG000 | 4 | 50 | 0.00 | 12.999 | 3 | 1 |
| P060EG000 | 4 | 60 | 0.00 | 12.998 | 3 | 1 |
| P070EG000 | 4 | 70 | 0.00 | 12.999 | 3 | 1 |
| P080EG000 | 4 | 80 | 0.00 | 12.996 | 3 | 1 |
| P085EG000 | 4 | 85 | 0.00 | 12.999 | 1 | |
| P090EG000 | 4 | 90 | 0.00 | 12.551 | 2 | |
| P095EG000 | 4 | 95 | 0.00 | 12.999 | 1 | |
| P0975EG000 | 4 | 97,5 | 0.00 | 12.999 | 1 | |
| P0995EG000 | 4 | 99,5 | 0.00 | 12.999 | 1 | |
| P100EG000 | 4 | 100 | 0.00 | 12.551 | 1 | |
| P070EG000 | 4 | 70 | 0.00 | 12.999 | 3 | 3 |
| P070EG025 | 4 | 70 | 0.25 | 13.000 | 4 | 3 |
| P070EG050 | 4 | 70 | 0.50 | 13.001 | 3 | 3 |
| P070EG075 | 4 | 70 | 0.75 | 13.003 | 4 | 3 |
| P070EG100 | 4 | | 1,00 | 13000 | 4 | 4 |

This figure shows the high level of reproducibility in results relative to the selected particle placement procedure (on this figure, like for the remainder of the article, the half-height of the vertical bars specific to points on the curves indicates the value of the standard deviation associated with these measurements) and demonstrates greater compactness for a mix containing 70% coarse particles and 30% fines, which is quite similar to what could be obtained in 3 dimensions **[4,9,10]**.

It should nonetheless be pointed out that the vast majority of models devoted to predicting minimum porosity $\eta_{min}$ indicate a continually decreasing porosity once any quantity of differently-sized parti-

**figure 8**
*Minimum porosity $\eta_{min}$ vs. mass proportion in coarse particles* p

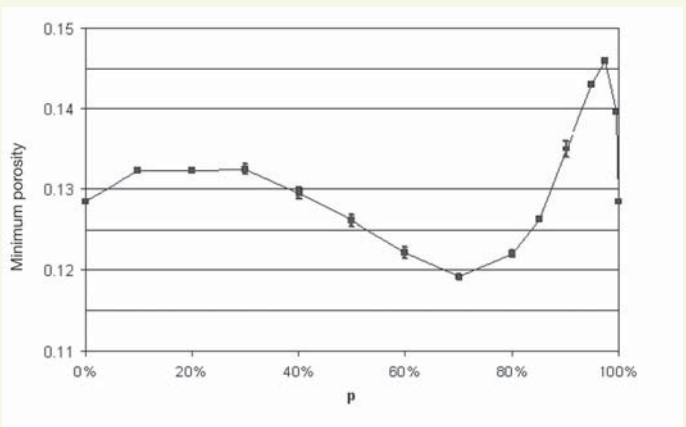

cles has been introduced into a homometric mix **(Fig. 2).** The observations provided herein however reveal a sharply higher minimum porosity, as a consequence of adding a few particles of a new type, than that potentially derived in the homometric mix. As shown in **Figure 3a**, the same-sized particle samples ($p = 0\%$ and $p = 100\ \%$) display a particle position pattern according to a triangular network. Introducing a small proportion of particles with relatively similar diameters into such a network disturbs the pattern quite significantly, thereby lessening the effects of both substitution and insertion.

The samples generated at an identical level of porosity (equal to the minimum porosity of a sample with a percentage $p = 30\%$, *i.e.* 0.134) display different density indices. The density indices defined in Equation **(10)** are presented for all test sample families on **Figure 9**.

**figure 9**
*Density index vs. mass proportion of coarse particles* p *for samples displaying the same porosity*

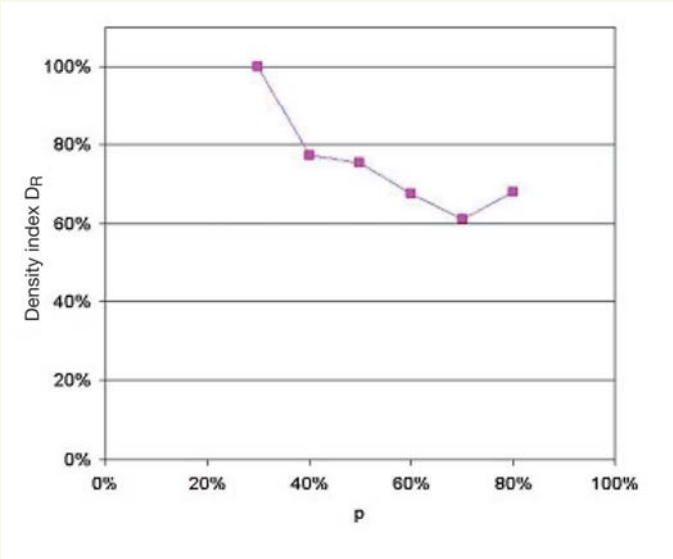


## › Intergranular orientation and number of contacts

The variations in global coordination number $Z$ (average number of contacts per particle in contact) vs. $p$ are shown in **Figure 10a**. The coordination number has been defined in this instance as the average number of contacts per particles containing at least two strictly positive forces. This number therefore excludes the so-called floating grains that carry no force, whose percentage within the various assemblies is depicted in **Figure 10b**.

As opposed to what is written in references **[7, 13, 21]**, granular assemblies at minimum porosity do not offer a constant average coordination number vs. proportion $p$ within a bimetric mix ($Z\sim4$ for $50< p< 90\%$; $Z\sim5$ for $p = 0\%$ and $p = 100\%$). The coordination number of an assembly of disordered discs cannot however exceed 4 within the limitation of stiff grains, regardless of the distribution of diameters. Coordination numbers greater than 4 are to be correlated with the crystalline appearance of the granular arrangement observed in broad zones of samples with a proportion $p$ not lying between 50% and 90%. In focusing on variations in the four partial coordination numbers (i.e. average number of contacts of a particle of type $i$ with particles of type $j$), the variations observed however are quite comparable to what has been given in references **[7, 13, 21]** **(Fig. 11)**.

From these curves, the maximum number of contacts that a single coarse particle could have among an arrangement of finer particles is deduced, i.e. 9 contacts (for 15 geometrically possible); conversely, a single fine particle within an arrangement of coarse particles would experience around three contacts (for 3 geometrically possible). In comparing the curves from **Figures 8** and **10**, it can

be stated, as has already been done **[13]**, that low porosity is not necessarily associated with high coordination number.

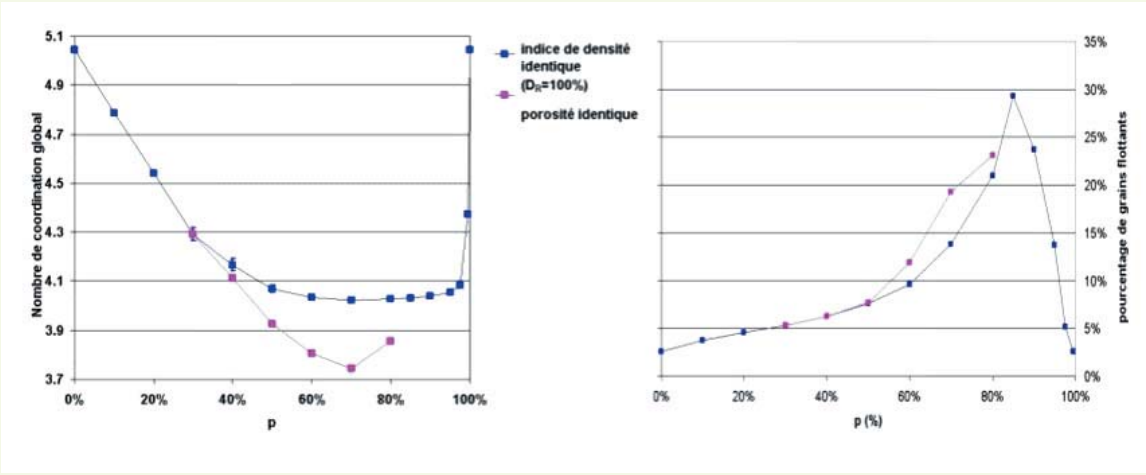


a | b

**figure 10**
*(a) Global coordination number and (b) percentage of suspended grains vs. the mass proportion of coarse particles* p, *for samples featuring the same density index ($D_R$ = 100%), minimum porosity or the same porosity*

To draw a conclusion regarding the granular arrangement of the studied assemblies, it is pointed out that the contact orientation of the assemblies exhibits good isotropy for mass percentages in coarse particles lying between 30% and 80%. Outside of this interval, the crystalline arrangement of fine particle assemblies would explain the preferred orientations of contacts at 0, 30, 60 and 90 degrees with respect to the partition direction **(Fig. 12)**.

For assemblies with the same porosity, it is noted that coordination number values oscillate between 3.75 and 4.27 **(Fig. 10)**. These numbers, some of which lie below 4, are correlated with the fact that during sample generation, the (nonzero) intergranular friction gradually diminishes until the correct porosity is ultimately reached; intergranular friction therefore is not equal to zero at the end of this phase.

For a given proportion *p*, the decrease in coordination number is tied to the decline in density index; the assembly characterized by *p* = 70% thus experiences the greatest drop in coordination number. It can then be expected that the mechanical properties of these assemblies within the domain of small deformations decrease more significantly in comparison with other samples.

**figure 11**
*Partial coordination numbers vs. mass proportion of coarse particles* p *for samples with minimum porosity (in acknowledging that grains carry zero force).* $C_{ij}$ *is the average number of contacts of particle* i *with particles of type* j*; index* P *denotes the smallest particles and* G *the largest (arrows indicate the axes pertinent to each curve).*

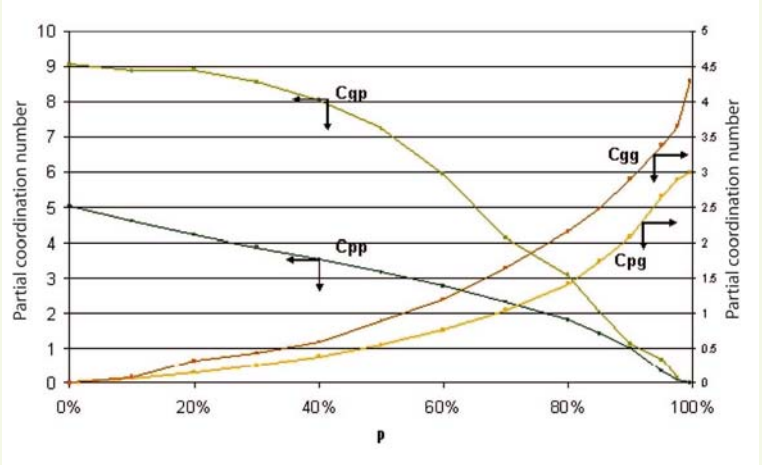

**figure 12**
*Distribution of contacts vs. their orientation, per angular category of 5 degrees (number of contacts per category / number of contacts for the perfectly-isotropic case), for assemblies: (a) p = 70 % at $D_R$ = 1 (b) p = 30 % at $D_R$ = 1.*

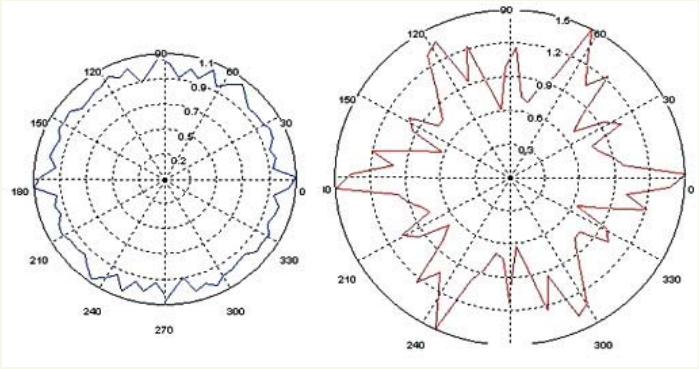


a | b

## Study of mechanical behavior under biaxial loading

A study of the mechanical behavior of this study's granular assemblies focuses primarily on the macroscopic response of samples subjected to biaxial loadings. The classical behavioral curve derived is presented in **Figure 13**:

The study pertains to three characteristic points:

– behavior in small deformations (calculated over an axial deformation interval ):

$2.10^{-5} < \varepsilon_1 < 2.10^{-4}$) :

- two-dimensional elasticity modulus $E_{2D} = \left.\frac{d(\sigma_1 - \sigma_3)}{d\varepsilon_1}\right|_{(\sigma_1 - \sigma_3) = 0}$ **(12)**,
- two-dimensional Poisson's ratio $\nu_{2D} = \left.\frac{d\varepsilon_3}{d\varepsilon_1}\right|_{\varepsilon_3 = 0}$, $0 \le \nu_{2D} \le 1$ **(13)**;

– behavior in large deformations:

- "characteristic state" **[22]**, angle of internal friction $\Phi_{carac}$ defined by $\frac{\sigma_1}{\sigma_3} = \tan^2\left(\frac{\pi}{4} + \frac{\varphi_{carac}}{2}\right)$ corresponding to $\frac{d\varepsilon_V}{d\varepsilon_1} = 0$ **(14)**
- "peak stress" state: angle of internal friction $\Phi_{peak}$ defined by $\frac{\sigma_1}{\sigma_3} = \tan^2\left(\frac{\pi}{4} + \frac{\varphi_{pic}}{2}\right)$ corresponding to $\dot{q} = 0$ **(15)**.

**figure 13**
*Behavioral curves of a sample under biaxial loading - Evolution of $(\sigma_1-\sigma_3)/\sigma_3$ and volumetric deformation $\varepsilon_V$ vs. axial deformation $\varepsilon_1$*

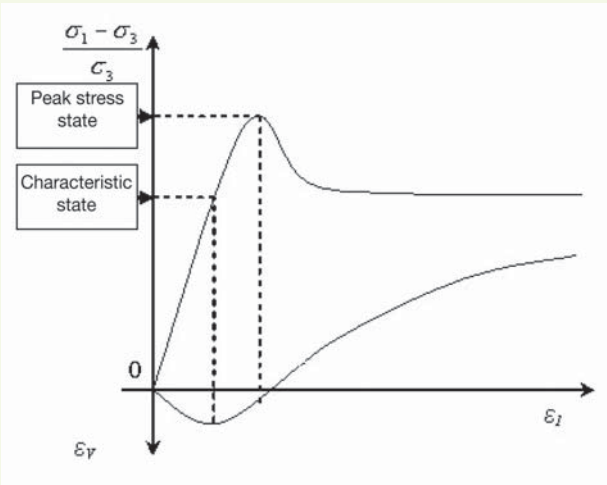

The entire series of granular assemblies generated and subjected to biaxial loading systematically exhibit contracting behavior within a narrow domain of axial deformation followed by a highly dilatant behavior. All of the curve-response $\frac{q}{\sigma_3} = \frac{\sigma_1 - \sigma_3}{\sigma_3} = f(\varepsilon_1)$ pairs display a peak stress **(Figs. 14** and **15)**.

**figure 14**
*Curves showing the evolution in $q/\sigma_3$ and volumetric deformation vs. axial deformation $\varepsilon_1$ of assembly P070EG000 (p = 70%) for two density indices ($\mu$ = 0.75)*

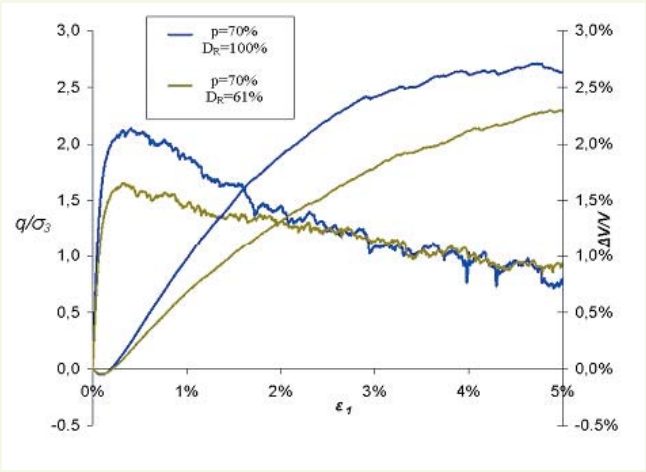


**figure 15**
*Curves showing the evolution in $q/\sigma_3$ and volumetric deformation vs. axial deformation $\varepsilon_1$ for various values of p and density index $D_R$ = 100%*

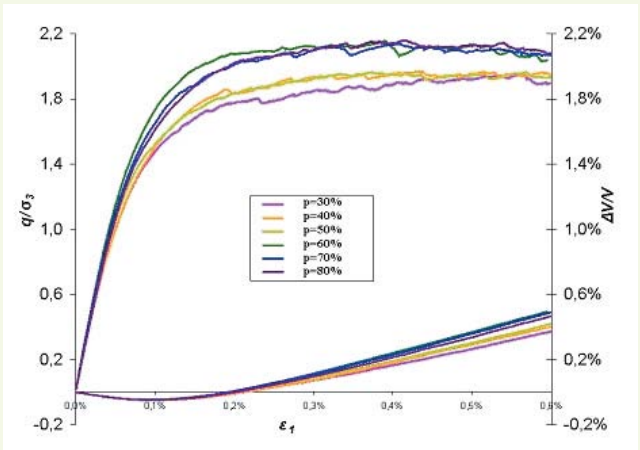


## › Domain of small deformations

The elastic properties of samples were obtained using a dynamic approach and then compared with the values yielded using a static approach **[16, 23]**. An example of such a comparison is provided in **Figure 16** below for a sample with proportion $p = 70\%$ and density index $D_R = 1$.

*Elasticity moduli*

The 2D elasticity moduli of samples at minimum porosity vary only slightly as a function of proportion $p$ (between 215 and 260 MPa) **(Fig. 17)**. In contrast, for assemblies with identical porosity, the assembly characterized by $p = 70\%$ leads, as could be expected and as mentioned above, to the lowest elasticity modulus value.

For assemblies at minimum porosity, no correlation between variations in global coordination number and elasticity modulus can be inferred from the results obtained **(Fig. 18a)**.

The assemblies displaying the greatest stiffness over the domain of small deformations are those whose mass proportion of coarse particles equals $p = 60\%$. On both sides of this pivotal $p$ value, the elasticity modulus drops. It can be remarked that adding a few fine particles into an assembly of

larger particles *(Z = 4.37)* seems to be more heavily penalizing in terms of elastic properties than adding a few large particles among finer particles *(Z = 4.70)*. Observation can nonetheless be made, within the limitation of disordered samples *(i.e. 50% < p < 90%)*, of a correlation between the 2D Young's modulus and the coordination number of the coarsest particles **(Fig. 18b).**

**figure 16**
*Comparison of the evolution in deviator* q *and volumetric deformation* $\Delta V/V$ *vs.* $\varepsilon_1$, *over the domain of small deformations by means of both a dynamic computation (PFC$^{2D}$) and static computation [16,23] for a sample of type P070EG000 (*p = 70%*) at density index* $D_R = 100\%$

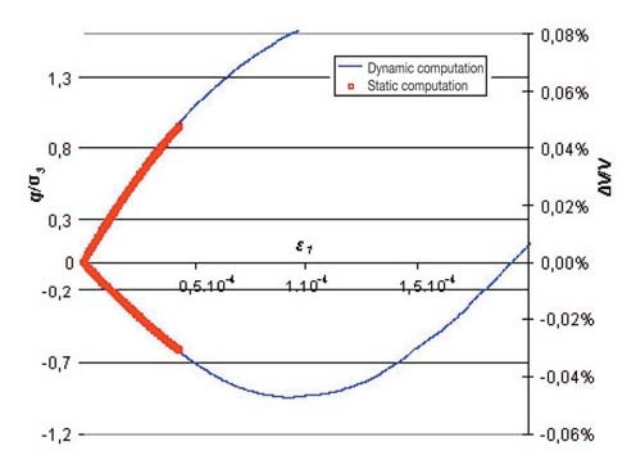


**figure 17**
*Evolution in elasticity modulus vs. p for samples with the same density index* ($D_R = 100\%$) *or at identical porosity*

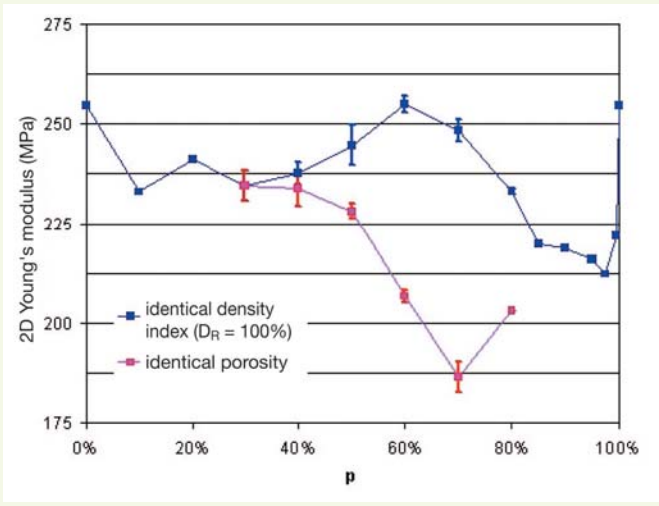


**figure 18**
*(a) Evolution in the 2D elasticity modulus of samples with an identical density index* ($D_R = 100\%$) *vs. their coordination number Z, (b) Evolution in the 2D elasticity modulus of disordered samples with an identical density index* ($D_R = 100\%$) *vs. coordination number of the coarsest particles*

a | b

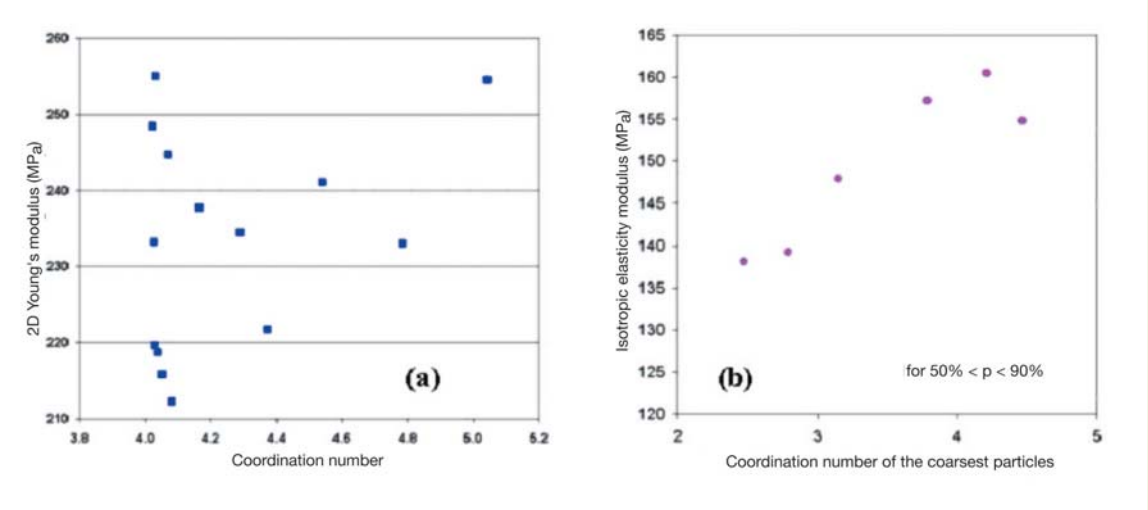

For assemblies at an identical porosity level, the fact of considering a porosity higher than their minimum causes a drop in elasticity modulus correlated with the density index. At a fixed porosity, the highest elasticity modulus is thus observed for the assembly featuring the greatest density index. In this case, a relation exists between the global coordination number and the elasticity modulus **(Fig. 19)**. As the contact network becomes denser, assembly stiffness rises.

*Poisson's ratios*

All other things being equal, the assemblies with a bimetric particle size distribution exhibit higher Poisson's ratios than the homometric assemblies **(Fig. 20)**. For mass percentages of coarse particles situated between 30% and 80%, the variations in Poisson's ratio remain extremely small (between 0.21 and 0.23), in comparison with those observed for all of the assemblies considered (between 0.16 and 0.23).

When assemblies have identical porosity, the Poisson's ratio increases to an even greater extent when deviating from the minimum porosity state. With a looser granular assembly, the Poisson's ratio rises. This result might seem to contradict what is observed classically for granular materials. Nonetheless, in limiting the domain to strictly elastic deformations, hence to a very low level of axial deformation ($10^{-5}$ to $10^{-4}$), this Poisson's ratio variation direction comes as no surprise. Triaxial tests conducted on sand and glass beads have revealed a drop in Poisson's ratio with porosity **[24]**.

**figure 19**
*Evolution in the 2D elasticity modulus of samples with an identical initial porosity vs. initial global coordination number*

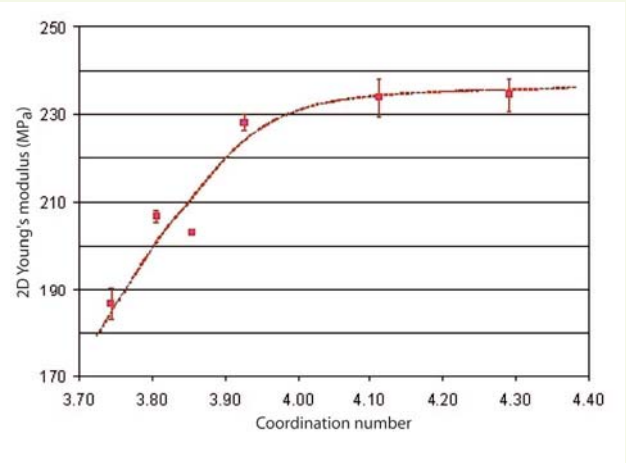


**figure 20**
*Evolution in the 2D Poisson's ratio of samples with an identical density index ($D_R$ = 100%) vs. their initial porosity*

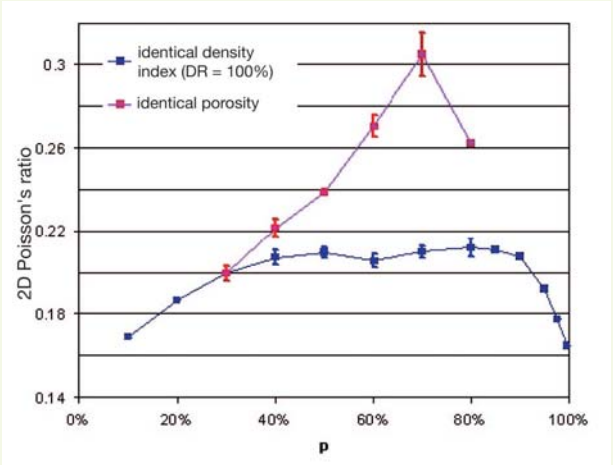

Moreover, this evolution is to be correlated with that for the number of contacts, which increases for the dense samples. Kuwano and Jardine **[25]** actually recorded a decline in Poisson's ratio when confinement pressure (hence number of contacts) rises. It has also been demonstrated that the *G/K* ratio (where *G* represents the shear modulus and *K* the isotropic compressive modulus of the assembly) increases with the coordination number **[26]** ($0 < G/K < 1$). Just like in two dimensions, the Poisson's ratio is correlated with the *G/K* ratio via the equation $\nu = \left(3 - 2\left(G/K\right)\right)/6$, and it may be concluded that behavior within the elastic domain of the studied granular assemblies fulfills expectations on this particular point.

## › Characteristic state

Biaxial tests were conducted beyond the domain of small deformations for mass proportions of coarse elements such that $30\% < p < 80\%$. The transition from contracting to dilatant behavior is revealed for very low axial deformation $\varepsilon_1$ values (between $8.5 \cdot 10^{-4}$ and $10^{-3}$). In considering the characteristic angle of friction values found for each granular distribution, the observation can be made that the characteristic state has been reached for deviatoric stress levels that rise even higher with initial sample density **(Fig. 21)**. It can thus be deduced that the characteristic state shows sensitivity to initial porosity, as opposed to what had been recorded with triaxial rotation loading under drained conditions subjected to constant confinement stress **[22, 27]**. This incompatibility does not imply a deviator level at the critical state that varies with porosity. The correspondence between characteristic state and critical state is not observed for the considered dense cylindrical assemblies.

## › Peak stress state

The peak stress is systematically encountered for $\varepsilon_1 < 7.10^{-3}$. In their minimum porosity state, granular assemblies featuring $30\% < p < 80\%$ show neighboring peak angles of friction at values between 30 and 31 degrees on average **(Fig. 22)**. The presence of considerable dispersion, which always exceeds the deviation between minimum and maximum observed values, merits attention.

As a consequence, it is difficult to draw a distinct trend regarding the influence of the proportions of bimetric mixes, introduced with minimum porosity, on shear strength characteristics.

In comparison with tests conducted at minimum porosity, the samples tested using initial states characterized by identical porosities lead to a decrease in peak angles of friction. This decrease is to be correlated with the drop in density index $D_R$ (*cf.* **Fig. 9**).

## › Conclusion

A mix of two particle families with each characterized by a single radius value, in comparison with a perfectly-homometric sample, causes strong modifications to the initial state under isotropic confinement. Variations in the mechanical behavior of assemblies with a given porosity are to be directly

**figure 21**
*Evolution in angle of friction equivalent to the characteristic state of samples with an identical density index ($D_R$ = 100%) vs. their initial porosity*

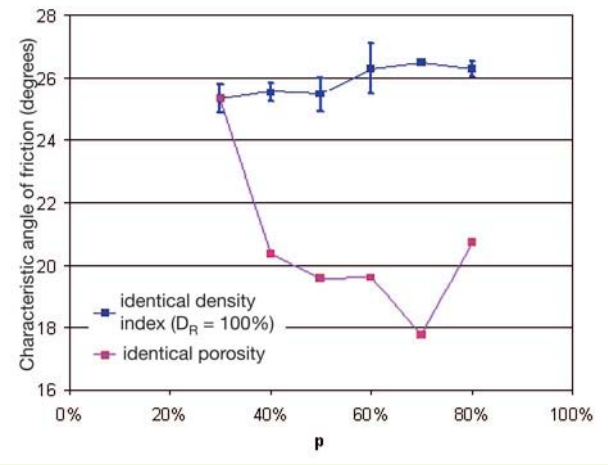

**figure 22**
*Evolution in angle of friction at sample peak stress with identical density index ($D_R$ = 100%) vs. their initial porosity*

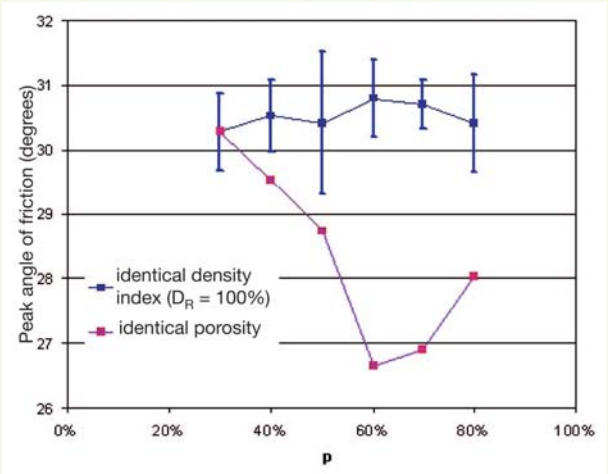


correlated with relative density indices of the initial state. At a constant density index ($D_R = 1$), the variations in mechanical characteristics of the bimetric assemblies are relatively limited, regardless of the mix proportions.

## INFLUENCE OF THE GRANULAR SPREAD OF MIX COMPONENT FAMILIES

### Initial state

The results presented below refer to the second series of samples composed of mixes with two particle families and a flat granular distribution. The granular spread of a given sample is characterized by the coefficient (*EG*), which is defined according to Equation **(11)**. At this point, it needs to be recalled that an assembly with a uniform particle size distribution possesses a granular spread of 1, whereas a bimetric assembly in which each component family contains same-sized particles has a zero granular spread.

As indicated previously, some samples were tested at minimum porosity and others at a given porosity level. In this latter case, the porosity is set equal to the minimum porosity of assemblies with granular spread *EG = 1* (i.e. continuous distribution), which yields the relative density indices shown in **Figure 23**.

**figure 23**
*Density index vs. granular spread EG for samples displaying the same porosity*

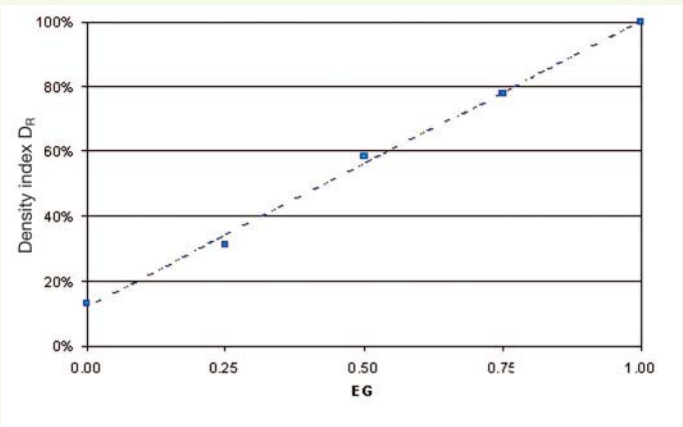

## › Study of porosity

In plotting the curve of minimum porosity vs. granular spread *EG*, it can be stated that the minimum porosity of a bimetric granular assembly drops even lower as the granulometric discontinuity rises **(Fig. 24)**.

**figure 24**
*Minimum porosity vs. granular spread EG*

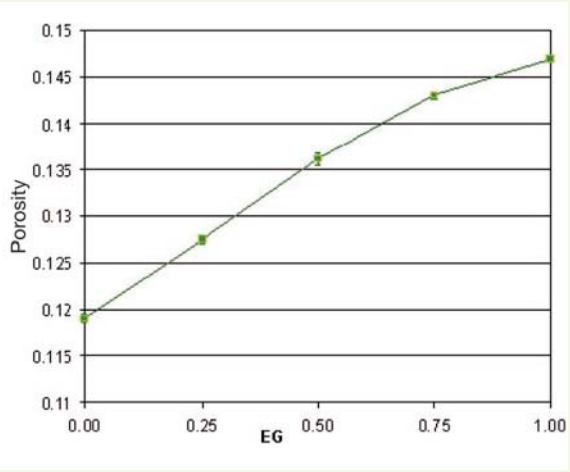


This result may be explained by considering our particle assembly to be a set of triangles formed by the centers of three connecting particles **[7]**. It can be observed that the triangular cells displaying the lowest porosity are those featuring differently-sized particles. As an example, in a granular mix composed of 70% by mass of particles with radius 4R (“G” particles) and 30% particles with radius R (“P” particles), the triangular cells generating the highest porosity are those composed of three “G” particles or three “P” particles. Their porosity lies on the order of 1.5 times greater than that of the other two cell types (PPG and PGG). This ratio increases with the radius ratio between “G” particles and “P” particles.

In the present case under study, as granular spread rises, the ratio between radii of particles forming a triangular cell becomes statistically weaker. As such, the minimum global porosity of the mix is higher. For a given mix with an extreme radius ratio, the minimum porosity would thus be smaller as the granular spread shrinks.

## › Intergranular orientation and number of contacts

The samples produced by means of coarsening without friction, i.e. at minimum porosity, offer a roughly constant global coordination number lying in the neighborhood of 4, which serves to confirm the absence of any regular arrangement between particles. A strong correlation can be noted herein between coordination number and relative porosity, both of which are constants **(Fig. 25)**.

In contrast, for assemblies with an identical porosity, a decrease in the average number of contacts is observed per particle that is even sharper with a lower density index. As the target porosity during sample creation deviates from the sample’s minimum porosity, the interparticle friction coefficient during assembly constitution actually rises, which consequently serves to limit the global number of contacts within the assembly, at a constant number of particles.

The orientation of contacts does not indicate any preferred direction, and this is so for all particle size distributions studied regardless of the relative porosity of the assembly under consideration.

**figure 25**
*Global coordination number vs. granular spread EG for samples with the same density index ($D_R$ = 100%) or at the same porosity level for* p = 70%

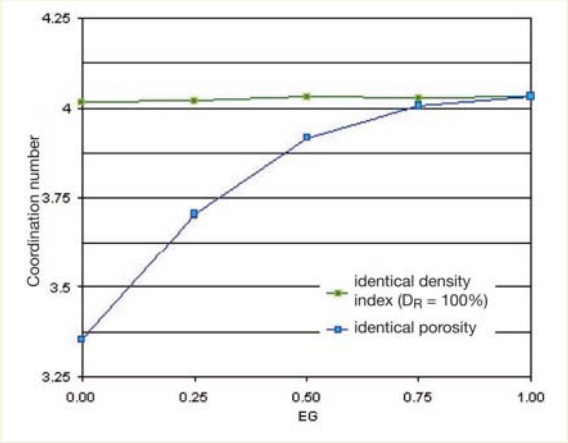


## Study of the mechanical behavior under biaxial loading

The global behavior of assemblies with variable granular spread is still characterized by an initial contracting phase observed for small axial deformations (less than 2.5‰), followed by a highly marked dilatancy phase **(Figs. 26** and **27)**.

### Domain of small deformations

*2D elasticity modulus*

Variations in elasticity modulus are heavily influenced by the initial porosity state. At minimum porosity, the 2D elasticity modulus actually decreases in accordance with the granulometric discontinuity (from 248 MPa for *EG = 0* to 215 MPa for *EG = 1*) **(Fig. 28)**. No correlation exists here between elasticity modulus and initial global coordination number however, as the latter remains constant.

On the other hand, when porosity is identical, the influence of density index can once again be seen. Elasticity modulus rises with granular spread and hence with the global coordination number of the assembly.

Beyond a granular spread of 0.5, the various particle size distributions are characterized by similar mechanical properties, tied obviously to the similarities in their initial state (minimum porosity, coordination number). The discontinuity effect is marked when granular spread drops below 0.5.

*2D Poisson's ratio*

The variations in 2D Poisson's ratio become more prominent as granular spread narrows **(Fig. 29)**. For *EG* values in excess of 0.5, the influence of granular spread is, like before,

**figure 26**
*Curves showing the evolution in $q/\sigma_3$ and volumetric deformation vs. axial deformation $\varepsilon_1$ for samples with P070EG050 (*p = 70% *and EG = 0.5) and for two density indices*

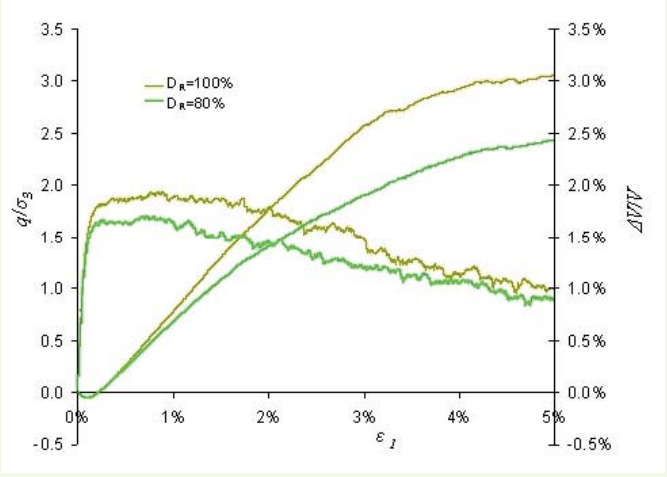

weak. In contrast, the decrease in density index of an assembly causes its Poisson's ratio to rise significantly.

**figure 27**
*Curves showing the evolution in $q/\sigma_3$ and volumetric deformation vs. axial deformation $\varepsilon_1$ for samples with a variable granular spread EG and for density index $D_R = 100\%$*

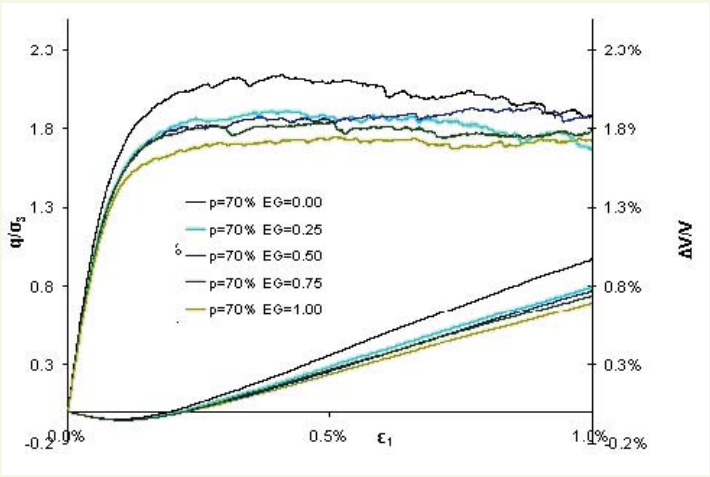


**figure 28**
*Evolution in the 2D elasticity modulus vs. granular spread EG for samples with the same density index ($D_R = 100\%$) or at the same level of porosity*

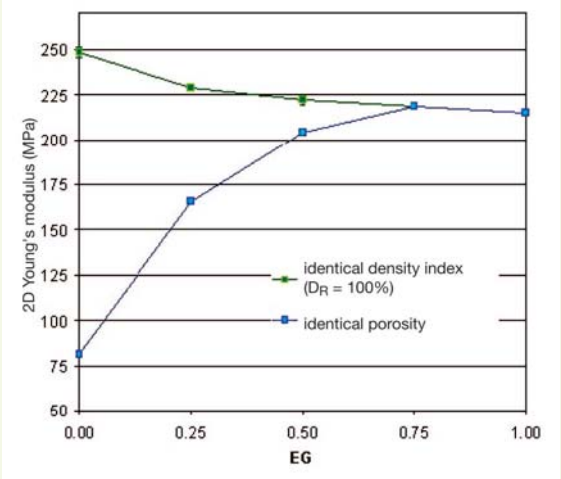


**figure 29**
*Evolution in the 2D Poisson's ratio vs. granular spread EG for samples with the same density index ($D_R = 100\%$) or at the same level of porosity*

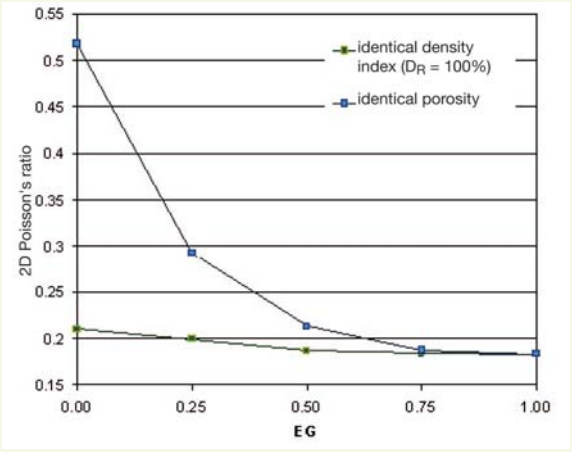


## › Characteristic state

The characteristic state is defined as a level of stress that may be quantified by means of an equivalent angle of friction $\dot{\varepsilon}_V = 0$. At minimum porosity, this deviator level is higher when granulometric

discontinuity is strong **(Fig. 30)**; in this case, the angle of friction at the characteristic state varies between $\phi_{carac} = 26.5$ *degrees* for $EG = 0$ and $\phi_{carac} = 25$ *degrees* for $EG = 1$.

The biaxial tests conducted on assemblies with the same initial porosity reveal a strong dependence between equivalent angle of friction at the characteristic state and initial porosity. The assemblies with zero granular spread, for which the difference in density index is greatest, indicate a drop in equivalent angle of friction at the characteristic state of $\phi_{carac} = 26.5$ *degrees* for a density index $D_R = 100\%$, at $\phi_{carac} = 12.1$ *degrees* for $D_R = 0.13$. The independence of characteristic state with respect to initial porosity has thus not been replicated.

The effect of granulometric discontinuity proves to be of little significance when granular spread lies above 0.5.

### › Peak stress state

The shear strength of assemblies, as characterized by the angle of friction at peak stress, follows variations analogous to those observed for the equivalent angle of friction at the characteristic state **(Fig. 31)**. When $D_R = 100\%$, shear strength increases as the granulometric discontinuity widens ($\phi_{peak} = 30.7$ *degrees* for $EG = 0$ vs. $\phi_{peak} = 28.2$ *degrees* for $EG = 1$). Moreover, the strong dependence with respect to density index has once again been demonstrated: at a zero granular spread, the shear strength falls to $\phi_{peak} = 19$ *degrees* for $\eta = 0.1465$.

**figure 30**
*Evolution in the angle of friction corresponding with the characteristic state vs. granular spread EG for samples with the same density index ($D_R = 100\%$) or at the same level of porosity*

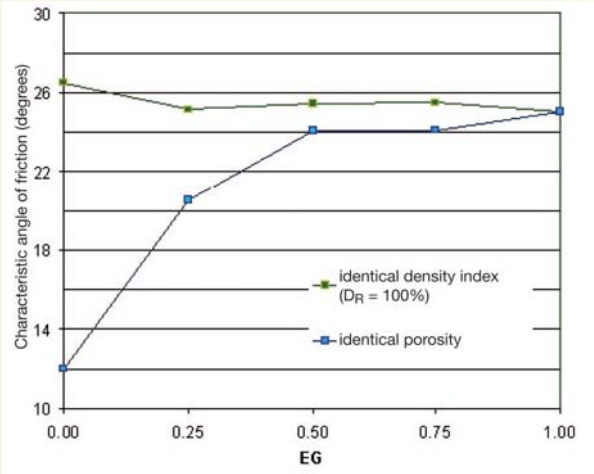


**figure 31**
*Evolution in the angle of friction at peak stress vs. granular spread EG for samples with the same density index ($D_R = 100\%$) or at the same level of porosity*

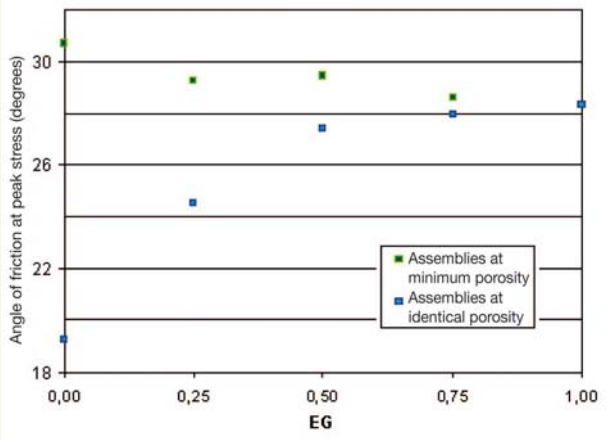

### › Conclusion

The study of relative size variation in the granulometric discontinuity has revealed the presence of a transition between the mechanical behavior of an assembly with continuous or uniform size distribution and an assembly displaying a distribution discontinuity. At an extreme radius ratio and equal density indices, mechanical properties are enhanced as the discontinuity heightens. Furthermore, when the magnitude of the discontinuity is less than half the deviation between extreme radii, assembly behavior is roughly the same as that of an assembly with a density index of 1.

## GENERAL CONCLUSION

Heterometric granular assemblies can be described using many structural parameters, in particular regarding their particle size distribution. The influence of two of these parameters, i.e. the proportion of coarse elements and granular spread, on the mechanical response of 2D particle assemblies submitted to biaxial loading have been qualitatively characterized herein. The two-dimensional numerical simulations presented were conducted on bimetric model materials (with two particle families, each characterized by a specific particle distribution). The parameters studied consisted of both the mass proportion $p$ of an assembly composed of larger-sized particles and the granular spread $EG$, which enables quantifying the granulometric discontinuity separating the two particle families.

The statistical study of samples exposed a remarkable value of the percentage mass in coarsest elements, $60 < p < 70\%$, for which the optimal porosity obtained also happens to be lowest. This result confirms the experimental results derived by P. Reiffsteck on glass bead assemblies **[5]**. It needs to be pointed out however that the number of discs not in contact, i.e. free within the assemblies, actually increases with proportion $p$ in order to reach a maximum of 30% for $p = 85\%$.

At the same time, it could be observed that for $60\% < p < 70\%$, the angles of friction at the characteristic state ( $\dot{\varepsilon}_v = 0$ ) and at peak stress ( $\dot{q} = 0$ ) are highest. Yet in considering the elastic phase of the behavior of these assemblies submitted to biaxial loading, the highest Young's modulus value is found for $p = 60\%$. Concerning the behavior of bimetric assemblies at minimum porosity, it was shown that mechanical characteristics only varied slightly, and this was so regardless of mix proportions. For samples with the same density index, no correlation was observed between coordination number and 2D elasticity modulus as $p$ varies, as opposed to the case of samples at the same level of porosity.

The study on the influence of granular spread indicates that minimum porosity is lower as the granulometric discontinuity widens.

As regards the mechanical response of these assemblies, two key elements should be emphasized. At the same density index, the spread in particle size distributions causes a systematic decrease in the mechanical properties measured (Young's modulus, characteristic and peak angles of friction). At the same initial porosity, the granulometric discontinuity of an assembly does not appear to influence the mechanical response, provided the granular spread remains above $EG = 0.5$. For $EG$ values of $< 0.5$, a drop in mechanical properties is recorded with granular spread, with the result needing to be placed in context with the decline in density index $D_R$.

The comparison of mechanical responses for the entire array of assemblies studied has revealed that the initial porosity and density index $D_R$ of samples are the structural parameters that exert a very considerable impact on the mechanical behavior of study samples.

The influence of the ratio between extreme particle radius values still needs to be quantified, especially for a radius ratio exceeding the threshold ratio $\alpha$ (2;3) ( $\alpha_{2D} = 6,46$ ). It would also be beneficial to examine the influence of granulometric discontinuities for other bimetric mix proportions (for purposes of this study, $p = 70\%$ was selected).

To obtain additional and more quantitative results, this study would need to be expanded to encompass model materials in three dimensions in order to assess the extent to which numerical simulations are able to reproduce the experimental triaxial tests on heterogeneous soils, as well as to conduct research on more specific structural mechanisms such as load transfer mechanisms, arch formation, swelling or even soil/inclusion interactions.


## ACKNOWLEDGMENTS

*This study was conducted within the LIRIGM Interdisciplinary Research Laboratory involving the fields of Geology and Mechanical Engineering at the University Joseph Fourier in Grenoble, before the authors joined the 3S-R Laboratory on January 1st, 2007.*


## REFERENCES


1 **Flavigny E.**, **Desrues J.**, **Palayer B.**, Note technique : Le sable d'Hostun « RF », *Revue Française de Géotechnique*, **1990**, **53**, pp. 67-70.

2 **O'Sullivan C.**, **Bray J.D.**, **Riemer M.**, Examination of the response of regularly packed specimens of spherical particles using physical tests and discrete simulations, *ASCE Journal of Engineering Mechanics*, **2004**, pp. 1140-1150.

3 **Lade P.V.**, **Nelson R.B.**, Modelling the elastic behaviour of granular materials, *International Journal for Numerical and Analytical Methods in Geomechanics*, **2005**, **11-5**, pp. 521-542.

4 **Dano C.**, **Hicher P.Y.**, Evolution of elastic shear modulus in granular materials along isotropic and deviatoric stress paths, *15th ASCE Engineering Mechanics Conference*, Columbia University, New York, NY, **June 2002**.

5 **Reiffsteck P.**, Caractéristiques mécaniques d'un sol hétérogène : compactabilité, déformabilité, rupture, *Etudes et Recherches des Laboratoires des Ponts et Chaussées, Sciences pour le Génie Civil*, Laboratoire central des ponts et chaussées, **2004**.

6 **ITASCA CONSULTING GROUP Inc.**, *Particles Flow Code in two dimensions : User's Manual*, **1999**.

7 **Dodds J.A.**, The porosity and contact points in a multi-component random sphere packings calculated by a simple statistical geometrical model, *Journal of Colloid and Interface Science*, **1980**, **77(2)**, pp. 317-327.

8 **Bernal J.D.**, **Mason J.**, Packing of Spheres : Co-ordination of randomly packed spheres, *Nature*, **1960**, **188**, pp. 910-911.

9 **Ben Aim R.**, **Le Goff P.**, Effet de paroi dans les empilements désordonnés de sphères et application à la porosité des mélanges binaires, *Powder Technology*, **1967**, **1**, pp. 281-290.

10 **Troadec J.-P.**, **Dodds J.A.**, Global geometrical description of homogeneous hard sphere packings, In : *Disorder and Granular Media*, D. Bideau & A. Hansen (Eds), **1993**, pp. 133-163.

11 **Ben Aim R.**, *Étude de la texture des empilements de grains. Application de la perméabilité des mélanges binaires en régime moléculaire, intermédiaire, laminaire*, Thèse d'état de l'université de Nancy, **1970**.

12 **Suzuki O.**, **Oshima T.**, Estimation of the co-ordination number in a multi-component mixture of spheres, *Powder Technology*, **1983**, **35**, pp. 159-166.

13 **Pinson D.**, **Zou R.P.**, **Yu A.B.**, **Zulli P.**, **Mac Carthy M.J.**, Coordination number of binary mixtures of spheres, *Journal of Physics D : Applied Physics*, **1998**, **31**, pp. 457-462.

14 **Allen M.P.**, **Tildesley D.J.**, Computer simulation of liquids, *Oxford Science Publications*, **1994**.

15 **Cundall P.A.**, **Strack O.D.L.**, A discrete numerical model for granular assemblies, *Géotechnique*, **1979**, **29(1)**, pp. 47-65.

16 **Combe G.**, *Mécanique des matériaux granulaires et origines microscopiques de la déformation*, **2002**, ERLPC, Si8, 165 pages.

17 **Roux J.-N.**, **Chevoir F.**, Simulation numérique discrete et comportement mécanique des matériaux, *Bulletin des laboratoires des ponts et chaussées*, **2005**, **254**, pp. 109-138.

18 **Combe G.**, **Roux J.-N.**, Discrete numerical simulation, quasi-static deformation and origin of strain in granular materials, Actes du *Colloque "Deformation characteristics of Geomaterials"*, Di Benedetto *et al.* (Eds), Balkema, **2003**, pp. 1071-1078.

19 **Lanier J.**, **Combe G.**, An experimental study of deformation in 2D granular media, In : E. Dembicki, J.L. Auriault and Z. Sikora (Eds), *International Workshop for Homogeneization, Theory of Migration and Granular Bodies*, **1995**, pp. 143-149.

20 **Thornton C.**, **Sun G.**, Axisymmetric compression of 3D polydisperses systems of spheres, In *Powder and Grains 93*, Balkema, Rotterdam, **1993**, pp. 129-134.

21 **Dodds J.A.**, **Kuno H.**, Computer simulation and statistical geometric model for contacts in binary random two-dimensional disk packings, *Nature*, **1977**, **266**, pp. 615-615.

22 **Luong M.P.**, Etat caractéristique du sol, *Comptes-rendus de l'Académie des Sciences*, **1978**, **287B**, pp. 305-307.

23 **Combe G.**, **Roux J.-N.**, Quasi-static deformation of granular materials (*en préparation)*.

24 **Sharifipour M.**, *Caractérisation des sols par propagation d'ondes - Analyse critique de la technique des bender-extender elements*, Thèse de l'école centrale de Nantes, **2006**.

25 **Kuwano R.**, **Jardine R. J.**, On the applicability of cross-anisotropic elasticity to granular materials at very small strains, *Géotechnique*, **2002**, **52(10)**, pp. 727-749.

26 **Wyart M.**, On the rigidity of amorphous solids, *Annales de Physique*, **2005**, **30(3)**, pp. 1-96.

27 **Rowe P.W.**, The stress-dilatancy relation for static equilibrium of an assembly of particles in contact, *Proceedings of the Royal Society A*, **1962**, **169(23)**, pp. 500-527.